Photocurrent Generation in Thin SnO_2 Nanocrystalline Semiconductor Film Electrodes from Photoinduced Charge-Separation State in Porphyrin−C_{60} Dyad

F. Fungo,[†] L. Otero,[†] C. D. Borsarelli,[‡] E. N. Durantini,[†] J. J. Silber,[†] and L. Sereno*,[†]

Departamento de Química y Física, Universidad Nacional de Río Cuarto, Agencia Postal N^ro 3, 5800 Río Cuarto, Argentina and Instituto de Ciencias Químicas, Facultad de Agronomía y Agroindustria, Universidad Nacional de Santiago del Estero, Av. Belgrano (s) 1912 (4200) Santiago del Estero, Argentina

Received: August 10, 2001; In Final Form: October 22, 2001

The generation of photoelectrical effects through the spectral sensitization of wide band gap (SnO_2) nanostructured semiconductor electrode by the excitation of a novel porphyrin−fullerene (**P**−$\mathbf{C_{60}}$) dyad is reported. **P**−$\mathbf{C_{60}}$ was synthesized from 5-(4-amidophenyl)-10,15,20-tris(4-methoxylphenyl) porphyrin (**P**) linked to 1,2-dihydro-1,2-methoxyphenyl [60]-61-carboxilic acid (**acid-**$\mathbf{C_{60}}$) by an amide bond. Anodic photocurrents and photovoltages are observed under visible irradiation of ITO/SnO_2/ **P**−$\mathbf{C_{60}}$ electrodes, although the porphyrin fluorescence is strongly quenched by the $\mathbf{C_{60}}$ moiety in the dyad. The photocurrent generation quantum yield of the dyad **P**−$\mathbf{C_{60}}$ is around twice higher than the yield of the porphyrin moiety at the same wavelength (Soret band). A mechanism involving the formation of an intramolecular photoinduced charge-transfer state is proposed to explain the efficiency in the generation of photoelectrical effect.

1. Introduction

Over the basis of modern organic chemistry, one approach to mimic the photosynthetic energy conversion system in nature is the use of complex synthetic molecular arrays containing chromophores, electron donors, and electron acceptors linked by covalent and noncovalent bonds.[1−4] The energy stored in this system as a photoinduced intramolecular charge-separation state can be converted in electric work through an external circuit in a suitable photoelectrochemical cell. The functionalization of C_{60} buckminsterfullerene[5,6] allows the linkage of this good energy and electron acceptor to many chromophores and has opened the possibility of constructing artificial photosynthetic systems in which there is a photoinduced electron or energy transfer process from a chromophore donor to a fullerene acceptor. On the other hand, many studies on the development of optoelectronic and energy conversion devices incorporate chlorophyll derivatives and several related metallized and unmetallized tetrapyrrolic compounds, as light receptors and charge storage units,[7−22] because of their remarkable optical and redox properties.[23−26] Thus, it is not surprising that great effort has been made in the synthesis and photophysical characterization of $\mathbf{C_{60}}$ covalently and noncovalently linked to porphyrins, for which quantum yields of photoinduced charge-separation state formation approaching one have been reported.[27−32] Moreover, solid-state double-layer photoelectrochemical cells were developed[33] and showed that the photoinduced electron transfer from porphyrin to $\mathbf{C_{60}}$ is the primary process of photocurrent generation at the porphyrin/$\mathbf{C_{60}}$ interface.

In the present work, we are interested in the use of a porpyrin−C_{60} dyad (**P**−$\mathbf{C_{60}}$, Figure 1) as a light receptor in the spectral sensitization of nanostructured tin oxide semiconductor electrode. In the sensitization of wide band gap semiconductors, the energy difference between the conduction band edge of an n-type semiconductor film and the oxidation potential of an excited dye present as an adsorbate provides a driving force for interfacial state charge injection.[34−36] However, only the dye directly adsorbed over the semiconductor produces a

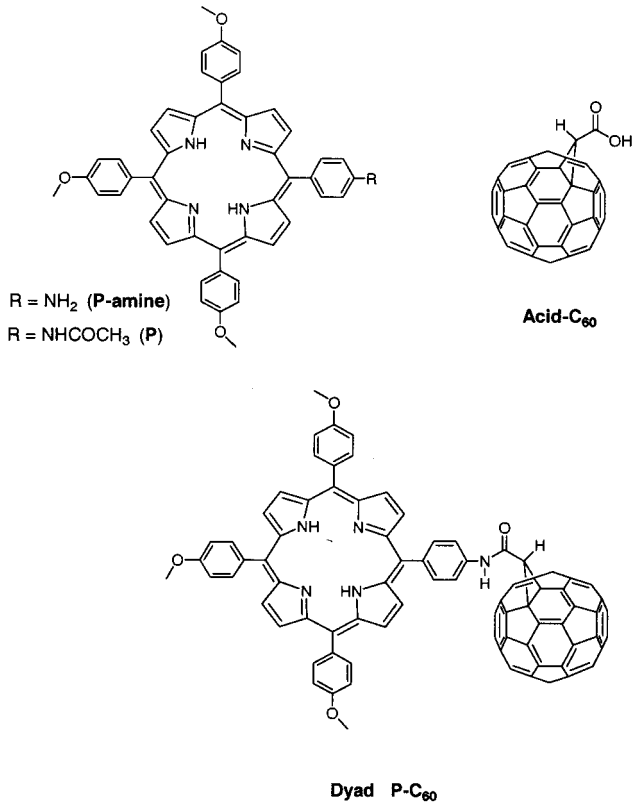

Figure 1. Structures of the dyad **P**−$\mathbf{C_{60}}$ and its monomers.

* To whom correspondence should be addressed. E-mail: sereno@arnet.com.ar.
[†] Universidad Nacional de Río Cuarto.
[‡] Universidad Nacional de Santiago del Estero.

10.1021/jp013113t CCC: $22.00
Published on Web 03/30/2002

significant photoelectrical effect, and the successive layers act as optical filter and electric insulator. Because the light-harvesting efficiency of a single monolayer is very low, the production of porous films of nanometer-sized semiconductor particles from colloidal suspensions is very useful because these films have large effective surface area, allowing substantial light absorption.[37−42] At the present, the spectral sensitization of porous metal oxides by adsorbed porphyrins has shown the production of light-harvesting and charge-separation efficiencies, in some cases comparable to those in natural photosynthesis, with a very high (nearly 80%) incident-photon-to-current efficiency (IPCE).[8]

On the contrary, the photoelectrical studies of fullerene films demonstrated very weak activity, mainly because of the problems related to the construction of relatively thick films able to absorb most of the incident light.[43] Nevertheless, the properties of devices involving the generation of excited state of fullerene are still extensively analyzed because of their potential use in optoelectronic and photovoltaic applications. We report here the efficient generation of photoelectrical effects in the spectral sensitization of SnO_2 nanostructured semiconductor electrodes from the excitation of both porphyrin and fullerene moieties in a **P−C$_{60}$** dyad, and a mechanism involving the formation of an intramolecular photoinduced charge-transfer state is proposed.

2. Experimental Section

Synthesis of Porpyrin−C$_{60}$ Heterodimer. The structure of the porpyrin−C_{60} dyad (**P−C$_{60}$**) and monomers moieties are shown in Figure 1. All the chemicals from Aldrich were used without further purification. 5-(4-Acetamidophenyl)-10,15,20-tris(4-methoxylphenyl) porphyrin (**P**) was prepared from the corresponding dipyrromethans by a procedure described before.[21,44] 4-Methoxylbenzaldehyde and 4-acetamidobenzaldehyde were reacted with *meso*-(4-methoxylphenyl) dipyrromethane in chloroform. The reaction was catalyzed by $BF_3 \cdot O(Et)_2$ at room temperature. The chlorin compounds were oxidized to the corresponding porphyrins with 2,3-dichloro-5,6-dicyano-1,4-benzoquinone (DDQ). Amide porphyrin (**P)** was purified by flash chromatography and basic hydrolysis of it afforded 5-(4-aminophenyl)-10,15,20-tris (4-methoxylphenyl) porphyrin (**P-amine**).

The precursor 1,2-dihydro-1,2-methanofullerene[60]-61-carboxylic acid (**C$_{60}$-acid**) was prepared according to the method described before in the literature.[45]

Porphyrin−C_{60} (**P−C$_{60}$**) dyad was obtained by the coupling reaction between **P-amine** and **C$_{60}$-acid** in dry bromobenzene. The reaction was performed in the presence of dicyclohexylcarbodiimide, 1-hydroxybenzotriazole, triethylamine, and 4-(dimethylamino) pyridine for 24 h at room temperature. The product was purified by flash column chromatography.[21] Spectroscopic data of the porphyrin derivatives coincide with those previously reported.[21]

Semiempirical molecular orbital calculations (AM1) were carried out using HyperChem software.[46]

Preparation of SnO_2 Nanocrystalline Films. The SnO_2 nanostructured film thin electrodes were prepared by using a modification of the Kamat's procedure.[11,47] As base contact, optically transparent electrodes of indium tin oxide (ITO, 100 Ω/square, Delta Technologies) were used. The ITO slides were cleaned by the method already described.[20]

ITO/SnO_2 electrodes were prepared by spin coating using a P6204-A model Specialty Coating System. Aliquots of 0.1 mL of SnO_2 colloidal suspension (1.5% SnO_2, particle diameter 20−30 Å, Alfa Chemicals) were spread onto clean ITO surfaces with a 3.5 cm^2 area and span at 3000 rpm for 30 s, then the electrodes were dried 5 min at 80 °C. Thick films of pristine SnO_2 were obtained by repeating the applications 15 times. The final films were annealed at 450 °C for 1 h.

ITO/SnO_2 electrodes were modified with **P−C$_{60}$** dyad and the porphyrin moiety (**P**) (Figure 1) by soaking ITO/SnO_2 films in a saturated *n*-hexane/dichloromethane (DCM Sintorgan HPLC grade) 70/30 solution of the dye for a period of 2 h. The electrodes, hereafter referred as ITO/SnO_2/ **P−C$_{60}$** and ITO/SnO_2/**P** electrodes, respectively, were then washed with the same solvent, dried in nitrogen stream at room temperature and stored in vials. ITO/SnO_2/ **C$_{60}$** electrodes were prepared by evaporation of the solvent of a DCM solution of C_{60} (0.1 mL 1×10^{-4} M) over a warm (∼40 °C) ITO/SnO_2 electrode. A copper wire was connected to the electrodes surface with an indium solder to achieve electric contact.

Absorption and Emission Spectroscopy. Absorption and emission spectroscopy of both **P** and **P−C$_{60}$** in solution (toluene; DCM and dimethylformamide, DMF) and in adsorbed state were analyzed using the previously described equipment.[20] Fluorescence quantum yield of porphyrin was calculated by steady-state comparative method using 5,10,15,20-tetraphenylporphyrin (TPP, $\Phi = 0.11$) as standard.[27]

Laser-Flash Photolysis Experiments. The laser-flash photolysis setup has been described elsewhere.[48] A Q-switched Nd:YAG laser (Spectron SL400) was used as the excitation source operating at 532 nm (20 ns halfwith) to excite the porphyrin moiety of the compounds. The laser beam was abated by using neutral filters to avoid multiphotonic processes and photodegradation of the samples. The sample solutions were matched in absorbance at 532 nm, the wavelength of the exciting laser pulse, within 5%. External electron acceptor (methyl viologen, MV^{2+} dichloride, Aldrich) was used as received.

Oxygen Molecular Singlet Measurements. Singlet molecular oxygen $O_2(^1\Delta_g)$ sensitization was measured by using time-resolved phosphorescence detection method (TRPD). The laser source was the same as the one used in the laser-flash photolysis experiments. The emitted radiation (mainly 1270 nm) was detected at right angles with an amplified Judson J16/8Sp germanium detector, after passing through appropriate filters to avoid residual fluorescence and scattered light.[49] The output of the detector was coupled to a digital oscilloscope (Hewlett−Packard HP-54504A). About twenty shots were usually needed for averaging decay times to get a good signal-to-noise ratio. The averaged signals were analyzed as single exponential decays by using a calculation software (Microcal Origin 4.1, Northampton, USA). The absorbances of the sample and reference were matched at the irradiation wavelength. Upon laser excitation of these solutions, the Φ_Δ value was obtained by comparison of the slopes of the linear plots of the initial extrapolated ($t = 0$ μs) 1270 nm $O_2(^1\Delta_g)$ luminescence versus the total laser energy.

Electrochemistry. Cyclic voltammetry (CV) was performed by using a potentiostat−galvanostat EG & G Princeton Applied Research PAR-273 and a low-volume Pyrex cell (V2 Cell, Bioanalytical Systems). The working electrode was a Pt disk of 0.031 cm^2. CV studies were carried out in 1,2- dichloroethane (DCE, Merck) containing 0.1 M tetrabutylammonium hexafluorophosphate (TBAHFP, Aldrich) as the supporting electrolyte. All the potentials were referred to a Ag/AgCl reference electrode and were corrected for IR drop by positive feedback technique.

Photoelectrochemical Measurements. Photoelectrochemical experiments were performed in 0.01 M aqueous solutions of hydroquinone (H_2Q, Aldrich, recrystallized from toluene), with

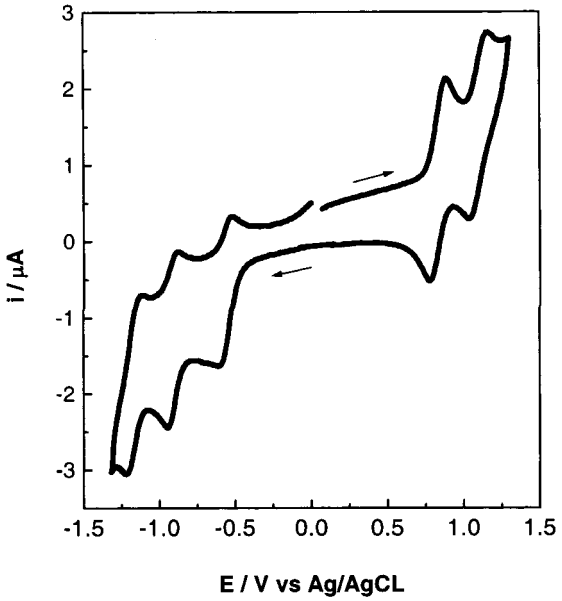

Figure 2. Cyclic voltammogram at a platinum electrode ($A = 0.031$ cm^2) of **P**−**C$_{60}$** 0.48 mM in DCE containing 0.1 M TBAHFP as supporting electrolyte, sweep rate = 0.100 V/s.

SCHEME 1

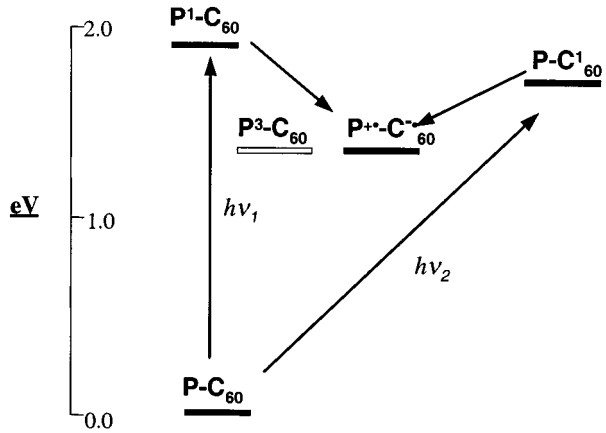

phosphate buffer (pH = 5.2) prepared from 0.05 M NaH_2PO_4 (Anedra > 99%) and NaOH (Baker). These solutions were degassed by bubbling with N_2 and maintained in the top of the cell by continuous stream. The measurements were carried out in an already described quartz photoelectrochemical cell using a homemade battery operated at low noise potentiostat.[20] Action spectra of ITO/SnO_2/dye were obtained by illumination of the photoelectrodes with monochromatic light in front face configuration[20] (illuminated area: 1 cm^2). The incident light intensities at different wavelengths were measured with a Coherent Laser-Mate Q radiometer (sensitivity 1 μW).

3. Results and Discussion

Electrochemistry. To evaluate the energy of the charge-separated state in **P**−**C$_{60}$** dyad (Scheme 1), it is necessary to know both the reduction potential of **C$_{60}$** and the oxidation potential of the porphyrin moiety. Consequently, the energy of the charge-separation state in **P**$^{+\bullet}$−**C$_{60}$**$^{-\bullet}$ has been estimated from cyclic voltammetric experiments of the dyad in DCE. Figure 2 is a typical result of anodic and cathodic scans of the dyad in DCE. The electrochemical reduction shows three one-electron processes in the potential range between −0.5 and −1.25 V versus Ag/AgCl, corresponding to the first two waves at −0.57 and −0.91 V to the formation of mono and dianion of **C$_{60}$** moiety, respectively,[27,50] and the one at −1.17 V to the formation of porphyrin anion. On the other hand, oxidation of dyad takes place at 0.86 V, corresponding to the porphyrin radical cation, and at 1.1 V, corresponding to the porphyrin dication formation. The fullerenes are not oxidized within spanned range. The reduction and oxidation potentials of the dyad are similar to those of the combined individual monomeric units, and the results allow to estimate the energy of the **P**$^{+\bullet}$−**C$_{60}$**$^{-\bullet}$ state, which is 1.43 eV above the dyad ground state.

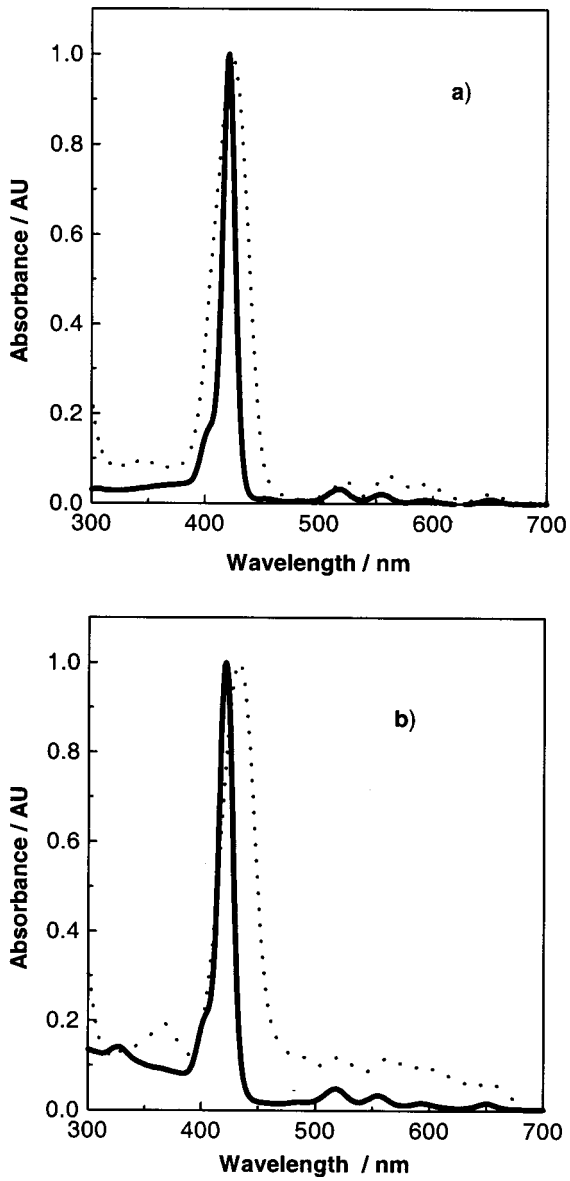

Figure 3. Absorption spectra of dyes in toluene solution (—) and in adsorbed state over ITO/SnO_2 electrodes (---). (a) **P**; (b) **P**−**C$_{60}$** dyad. Absorbances have been normalized to one.

Absorption and Fluorescence Spectra in Solution. The absorption spectra of both **P** and **P**−**C$_{60}$** compounds in toluene solution are shown in Figure 3. As can be observed, the spectrum of the dyad features four Q-band (λ_{max} = 518, 555, 593, and 650 nm), whereas the Soret band appears as a single maximum at 422 nm. The spectrum of the amido-porphyrin **P** exhibits Soret absorption at 422 nm and Q-band maxima at 518, 556, 594, and 651 nm. Thus, the lack of spectral perturbations in the dyad indicates a weak electronic interaction between the porphyrin and fullerene chromophores.[21]

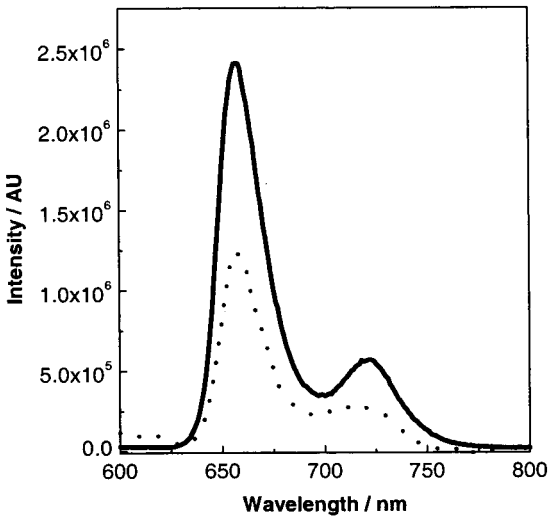

Figure 4. Corrected fluorescence emission spectrum of **P** (—) and **P**−**C**$_{60}$ dyad (····· x 25) in toluene. The absorbance of the dyes has been matched at the excitation wavelength, $\lambda_{ex} = 555$ nm.

The fluorescence emission spectra of both **P** and **P**−**C**$_{60}$ were measured in toluene. Typical results are shown in Figure 4. The amido-porphyrin **P** features fluorescence maxima at 658 and 722 nm, with a fluorescence quantum yield of ϕ_f**P** = 0.19 in deoxygenated toluene. On the other hand, the **P**−**C**$_{60}$ dyad in the solvent shows a much weaker emission from its porphyrin moiety (fluorescence quantum yield ϕ_f**P**−**C**$_{60}$ = 3.4×10^{-3}), indicating a strong quenching of the porphyrin excited singlet state (quenching efficiency, $\eta_q \geq 0.98$) by the attached fullerene. It would be reasonable to assume that the observed fluorescence quenching in nonpolar solvent could be due to singlet−singlet energy transfer from the porphyrin moiety to fullerene.[27−31] The energy of the fullerene moiety first excited singlet state is 1.77 eV, on the basis of the absorption and emission spectra of the model fullerene (Figure 1); meanwhile, the porphyrin first excited singlet state in the dyad (as calculated from the average of the frequencies of the longest wavelength absorption maxima and the shortest wavelength emission maxima) is 1.90 eV over the ground state (Scheme 1). However, since no evidence of fullerene fluorescence above 700 nm[27] was detected, the quenching of the porphyrin fluorescence observed in the dyad may not be all ascribed to an energy-transfer mechanism from the porphyrin excited state to the fullerene moiety. In fact, the shape of the normalized fluorescence spectra of **P**−**C**$_{60}$ is identical to that observed for **P**. (Figure 4)

Triplet−Triplet Transient Absorption Spectra. The transient absorption spectra obtained upon laser excitation at 532 nm of the amido-porphyrin **P** and for **P**−**C**$_{60}$ in degassed toluene solutions were almost the same and showed the typical feature of the porphyrins T−T spectra (Figure 5). In DMF solutions, the shape of the transient spectra of **P**−**C**$_{60}$ remains the same as for **P**, but for the dyad the amount of triplet state is reduced by a factor of 3, relative to that observed for **P**. In all the cases, the characteristic absorption at 690 nm assigned to the fullerene triplet state was not observed.

As was mentioned before, for the **P**−**C**$_{60}$ dyad in a nonpolar medium as toluene, more than 98% of the singlet state of the porphyrin moiety is quenched. However, the T−T absorption spectrum of **P**−**C**$_{60}$ shows that the efficiency of formation of the porphyrin triplet state is almost the same as for **P**. These results suggest the enhancement of the intersystem crossing by charge-transfer interactions.[51,52] This mechanism is favored when the free energy of the radical ion pair is greater than the lowest

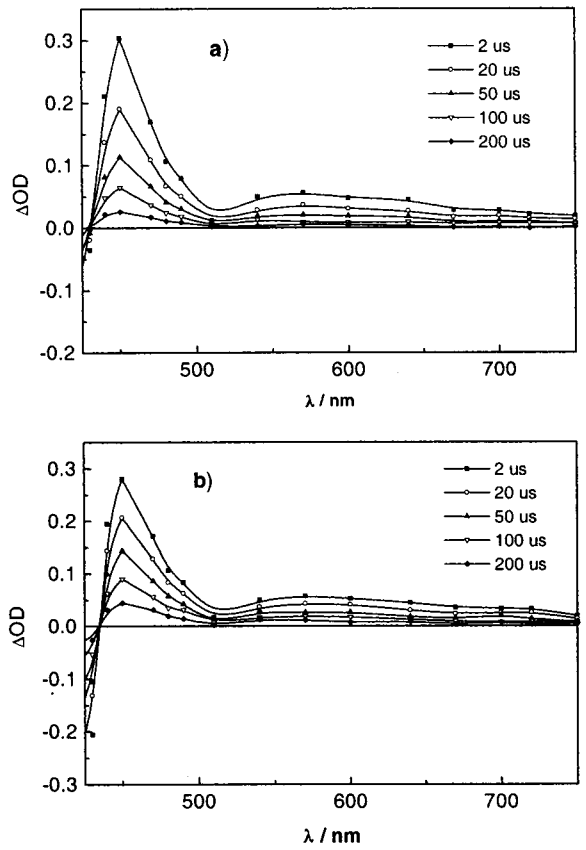

Figure 5. Transient absorption spectra obtained upon laser excitation at 532 nm of (a) **P** and (b) **P**−**C**$_{60}$ dyad in degassed toluene solutions. (Solutions have the same absorbance at the pump wavelength.)

molecular triplet energy.[51,52] The electrochemical measurements in DCE yielded ca. 1.43 eV for the energy of the **P**$^{+\bullet}$−**C**$_{60}^{-\bullet}$ state (see above), and it is known that the triplet state of a typical *meso*-tetraarylporphyrin such as **P** lies at about 1.44 eV.[53] Therefore, in a nonpolar solvent such as toluene, the charge-transfer state for **P**−**C**$_{60}$ should be at an energy >1.44 eV, allowing the increment of the intersystem crossing pathway by charge-transfer recombination. Since the energy of the **C**$_{60}$ triplet state is 1.55 eV,[54] the favored triplet state formed upon charge-transfer recombination is ^{3}**P**−**C**$_{60}$ instead of **P**−^{3}**C**$_{60}$. Recombination of photoinduced charge-separation states to triplet have been observed in other porphyrin−fullerene dyads[55,56] and caroteno−porphyrin−fullerene triads with high quantum yield.[57] Such effect was attributed in part to the low reorganization energy (λ) in the fullerene system.[57,58,63]

In more polar solvents such as DMF, the stabilization of the charge-transfer state **P**$^{+\bullet}$−**C**$_{60}^{-\bullet}$ at energy values below the porphyrin triplet state occurs, decreasing the efficiency of formation of the porphyrin triplet state from charge-transfer recombination. Unfortunately, our laser-flash photolysis setup (>50 ns, <800 nm) did not allow direct transient detection of the charge-transfer state **P**$^{+\bullet}$−**C**$_{60}^{-\bullet}$. However, the solvent effect upon the T−T spectra of **P**−**C**$_{60}$ seems to indicate that effectively a transient charge-transfer state is formed.

To confirm the formation of the charge-transfer state **P**$^{+\bullet}$−**C**$_{60}^{-\bullet}$, the addition of external electron acceptor (methyl viologen, MV^{2+} in water) to a **P**−**C**$_{60}$ DMF solution allows one to observe the formation of the reduced radical cation $MV^{+\bullet}$, in the transient spectra at 100 μs after 532 nm laser excitation (Figure 6). Intermolecular electron-transfer process from **C**$_{60}^{-\bullet}$ moiety of the photogenerated **P**$^{+\bullet}$−**C**$_{60}^{-\bullet}$ ion pair to MV^{2+} produces the generation of $MV^{+\bullet}$. This process

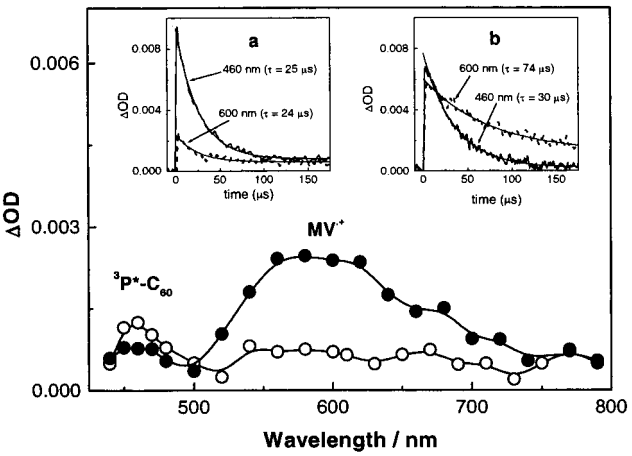

Figure 6. Transient absorption spectra of **P**−$\mathbf{C_{60}}$ obtained at 100 μs after the 532-nm laser pulse in DMF solutions (5% water) in (○) absence of MV^{2+} cation and (●) presence of 5 mM of MV^{2+} cation. Insets: decay curves at 460 and 600 nm in (a) absence of MV^{2+} cation and (b) presence of 5 mM of MV^{2+}.

competes with the back charge-transfer recombination of $\mathbf{P}^{+\bullet}-\mathbf{C_{60}}^{-\bullet}$ to yield $^3\mathbf{P}-\mathbf{C_{60}}$ state, as observed by lower T−T absorption in the presence of MV^{2+}. The insets in Figure 6 show the difference in the decays times of the porphyrin triplet state (clearly distinguished at 460 nm) and $MV^{+\bullet}$ cation (at 600 nm) confirming the different kinetic fate of both transient species. The results reinforce our proposition about the formation of the photoinduced charge-separated state in porphyrin−fullerene dyad. Imahori et al. observed similar intermolecular electron transfer[59] using a ferrocene−porphyrin−fullerene triad (Fe−P−C_{60}), the photoinduced $Fe^{+\bullet}-P-C_{60}^{-\bullet}$ state in benzonitrile was able to transfer an electron from $C_{60}^{-\bullet}$ to a hexyl viologen in solution.

Singlet Oxygen Molecular $O_2(^1\Delta_g)$ Photosensitization. In absence of an external electron donor or acceptor species, the excitation of the porphyrin moiety of the **P**−$\mathbf{C_{60}}$ dyad in fluid solution yields the $^3\mathbf{P}-\mathbf{C_{60}}$ as the main transient product. In presence of molecular oxygen, it is well known that the excited triplet state of porphyrins yields singlet molecular oxygen $O_2(^1\Delta_g)$ by an energy transfer.[60] Figure 7 shows the variation of the initial intensity ($t = 0$ μs) at 1270 nm of $O_2(^1\Delta_g)$ versus the total laser energy for **P** and **P**−$\mathbf{C_{60}}$ in toluene and DMF aerated solutions. In agreement with the results obtained with the T−T transient absorption spectra of **P** and **P**−$\mathbf{C_{60}}$, the photosensitization efficiency for $O_2(^1\Delta_g)$ for both compounds is similar in toluene, but in DMF the relative efficiency of **P** is 4 times higher than for **P**−$\mathbf{C_{60}}$(see above). These results confirm that the yield of the $^3\mathbf{P}-\mathbf{C_{60}}$ is very sensitive to the solvent polarity because it is originated from the charge-transfer separation state $\mathbf{P}^{+\bullet}-\mathbf{C_{60}}^{-\bullet}$.

Taking in account the observed results and by analogy with other porphyrin−fullerene dyads,[27,31] we can conclude that a photoinduced intramolecular electron transfer occurs in **P**−$\mathbf{C_{60}}$ arising from $^1\mathbf{P}-\mathbf{C_{60}}$ state. As shows in Scheme 1, $\mathbf{P}^{+\bullet}-\mathbf{C_{60}}^{-\bullet}$ state lies at about 0.47 eV below $^1\mathbf{P}-\mathbf{C_{60}}$.

It is interesting to compare our results with those observed for other porphyrin−fullerene dyad systems linked by different bridges,[27,61−63] where quantitative singlet−singlet energy transfer was detected. In these systems, strong electronic coupling between the moieties was observed, producing deformation and shift of the absorption bands in the UV−visible spectrum. These effects were related to the spatial architecture of the dyads, where the separation between the porphyrin and fullerene moieties is small. To gain an idea of this distance in **P**−$\mathbf{C_{60}}$ dyad, AM1 calculation was performed (constraining the geometry to obtain a planar structure in the porphyrin ring). After geometry optimization, a structure (Figure 8) where the center-to-center separation is about 14 Å is obtained. This is a quite larger distance than in those porphyrin−fullerene dyads where energy-transfer quenching of the porphyrin fluorescence was observed.[27]

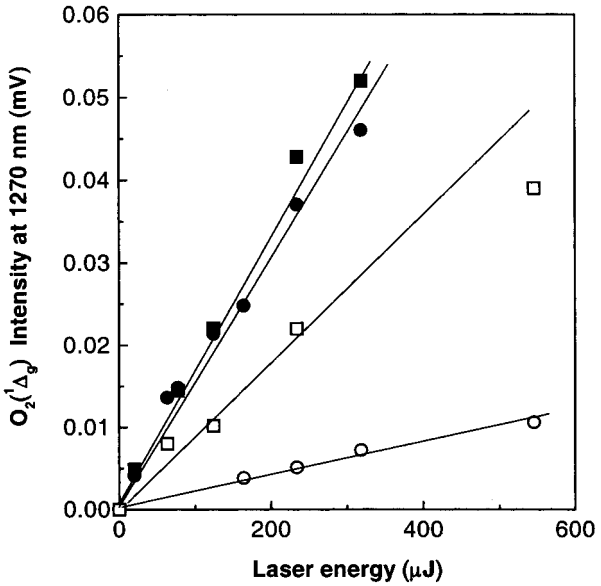

Figure 7. Emission intensity of O_2 ($^1\Delta_g$) at 1270 nm generated by excitation of **P** (squares) and **P**−$\mathbf{C_{60}}$ dyad (circles) in toluene (fill) and DMF (open) as function of the laser intensity. Laser irradiation wavelength 532 nm.

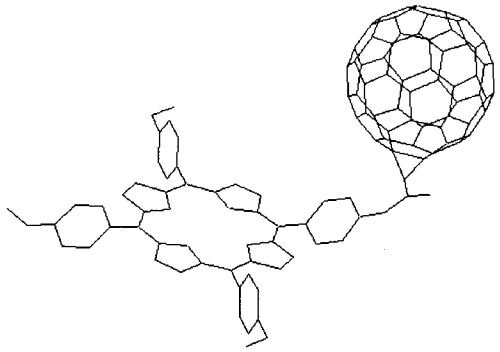

Figure 8. Schematic representation of the spatial conformation of the **P**−$\mathbf{C_{60}}$ dyad obtained from AM1 calculations.

Absorption and Emission Spectra of ITO/SnO_2/Dye Electrodes. Both amide porphyrin **P** and **P**−$\mathbf{C_{60}}$ dyad adsorption onto the semiconductor produces violet-green coloration of the electrodes. The electronic spectra of **P** and **P**−$\mathbf{C_{60}}$ dyad adsorbed on ITO/SnO_2/dye electrodes are shown in Figure 3. As can be observed, the amide porphyrin, when it is placed into SnO_2 film, shows only a small red shift (2 nm) at the Soret band with respect to toluene solution. On the other hand, in ITO/SnO_2/**P**−$\mathbf{C_{60}}$ electrodes, the porphyrin moiety Soret band is shifted 11 nm as compared to those in toluene solutions. This effect was also observed by Tkachenko et al.[64] for structurally related pophyrin−fullerene dyad in microcrystalline state and in Langmuir−Blodgett films, and it was attributed to the formation of an intermolecular complex between the porphyrin and the $\mathbf{C_{60}}$ moieties in the solid state. The absorption band at $\lambda_{max} = 367$ nm arising from the $\mathbf{C_{60}}$ moiety is clearly observed in ITO/SnO_2/**P**−$\mathbf{C_{60}}$electrode, but it is ∼30 nm red shifted with respect to the toluene solution.

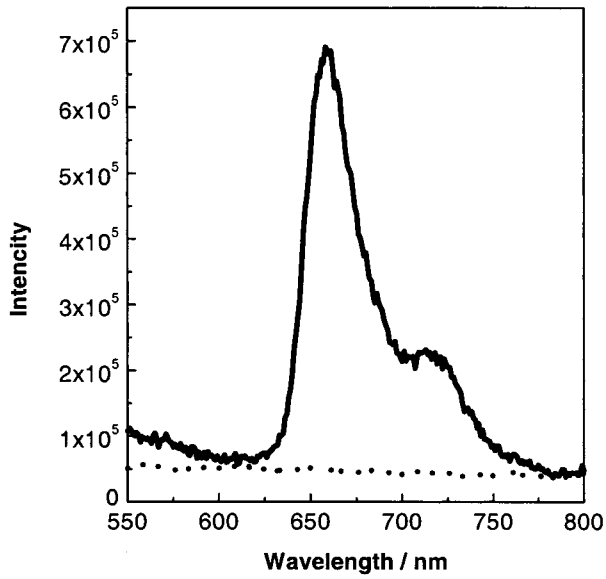

Figure 9. Corrected fluorescence emission spectrum of ITO/SnO_2/**P** (—) and ITO/SnO_2/**P**−**C60** (·····) λ_{ex} = 555 nm.

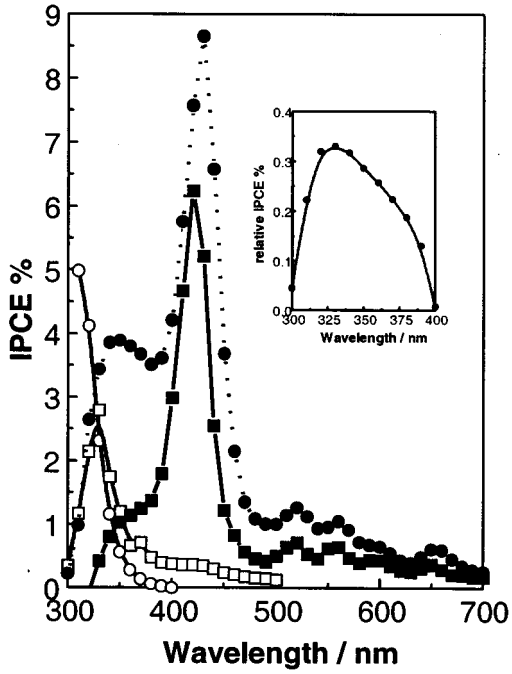

Figure 10. Action spectra as incident-photon-to-current efficiency, IPCE (%), of ITO/SnO_2 (x 4, open circles) and ITO/SnO_2/dye electrodes modified with **C60** (x 4, open squares); **P** (fill squares); and **P**−**C60** (fill circles) dyad. The inset shows the subtraction between the action spectra of the last two electrodes after normalization at the Soret bands.

The emission spectra of ITO/SnO_2/**P** and of ITO/SnO_2/**P**−**C60** electrodes are shown in Figure 9. As it can be seen, no significant emission from the **P** moiety occurs in the dyad, suggesting that electron transfer from the **P** to **C60** takes place also when the dyad is adsorbed on the electrode.

Photoelectrochemistry. The ITO/SnO_2/**P**−**C60** electrodes are photoelectrochemically active in the range between 300 and 700 nm (Figure 10). The generated photocurrent is anodic, and negative open circuit photopotentials are observed upon excitation, indicating that the electrons flow from the solution to ITO base contact through the illuminated electrode. The photocurrent is reproducible under several (hundreds) repeated on−off illumination cycles.

SCHEME 2

$$\mathbf{C_{60}} \xrightarrow{h\nu} {}^1\mathbf{C_{60}} \quad \text{(a)}$$

$${}^1\mathbf{C_{60}} + H_2Q \longrightarrow \mathbf{C_{60}}^{\bullet-} + HQ^{\bullet} + H^+ \quad \text{(b)}$$

$$\mathbf{C_{60}}^{\bullet-} + SnO_2 \longrightarrow \mathbf{C_{60}} + SnO_2(e^-) \quad \text{(c)}$$

Photocurrent Action Spectra. The incident-photon-to-photocurrent efficiencies (IPCE) for the ITO/SnO_2/**P**−**C60**, ITO/SnO_2/**P**, and ITO/SnO_2/**C60** electrodes were evaluated through eq 1.[47,65]

$$\text{IPCE (\%)} = 100\,(i_{sc}\,1240)/(I_{inc}\,\lambda) \qquad (1)$$

where i_{sc} is the short circuit photocurrent (A cm^{-2}), I_{inc} is the incident light intensity (W cm^{-2}), and λ is the excitation wavelength (nm). After subtraction of the photocurrent response of bare ITO/SnO_2 electrodes, recorded before dye modification, the action spectrum for the amide porphyrin and the dyad modified electrodes closely matches the absorption spectrum of the corresponding dye, as is shown in Figure 10. On the other hand, the photocurrent spectra obtained with ITO/SnO_2/**C60** electrodes showed only a small difference with those resulting from the band gap excitation of the SnO_2 film, indicating that in these experimental conditions direct excitation of fullerene is not able to produce significant photoelectric effects. The photocurrent generation in the last case probably involves a photogalvanic type behavior, where the excited **C60** takes one electron from the sacrificial donor (H_2Q) present in the solution to form fullerene anion, which then transfers one electron to SnO_2 conduction band (Scheme 2).

This kind of mechanism was already proposed for the observed anodic photocurrent generation in **C60** Langmuir−Blodgett monolayers ITO modified electrodes[66,67] and in **C60** cluster aggregates on nanostructured SnO_2 films.[43] This mechanism possesses the advantage that the back electron transfer (the reverse process for step c in Scheme 2) would require for the difficult reduction of a neutral species, while in most of the reported spectral sensitization processes the back electron transfer (which precludes the efficient generation of photocurrent) involves the cation of the dye.[34,35] The photosensitization mechanism involving direct charge injection from excited fullerene into SnO_2 nanocrystallites can be ruled out through the energetic analysis. **C60** oxidation is difficult, (gas-phase ionization potential was measured to be ca. 7.6 eV[68]), and the oxidation potential of **C60** ground state is ∼1.76 V versus SCE.[50,69] Taking the energy of the 0−0 electronic transition as 1.77 eV, the oxidation of **C60*** should occur at ∼(−0.01 V) versus SCE. As the flat band potential of the semiconductor is ∼(−0.2 V) versus SCE,[47] photoinduced charge transfer from excited fullerene into SnO_2 is an endergonic process.

On the other hand, in the action spectrum obtained with ITO/SnO_2/**P**−**C60** electrode, efficient generation of photocurrent at around λ = 350 nm is observed (Figure 10). This photocurrent is mainly produced by excitation of the **C60** moiety, as can be concluded from the analysis of the absorption spectrum of the dyad. In the inset of Figure 10, where the normalized to one (Soret band) action spectra of ITO/SnO_2/**P**−**C60** and ITO/SnO_2/**P** electrodes have been subtracted, the photocurrent generated by direct excitation of the **C60** moiety in the dyad molecule is clearly distinguished. Over the basis of the already described photogalvanic mechanisms[43,66,67] and the photophysical properties of the **P**−**C60** dyad, it is possible to propose that the photoelectric effects produced when the ITO/SnO_2/**P**−**C60**

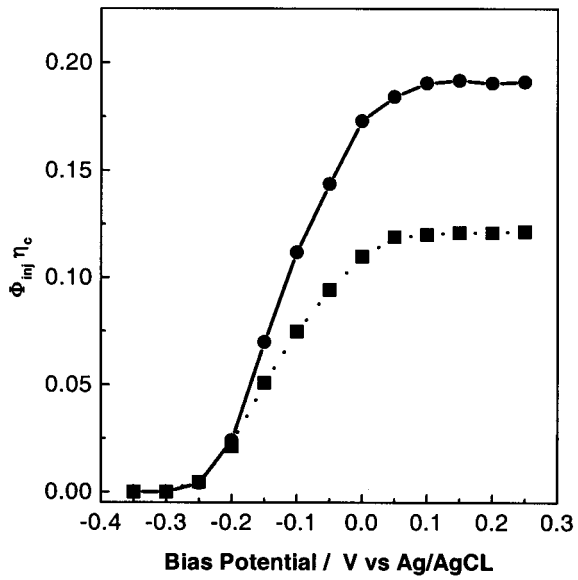

Figure 11. Dependence of the product of the charge injection yield (Φ_{inj}) and charge collection efficiency η_c at the maximum of Soret bands of ITO/SnO_2/**P**−$\mathbf{C_{60}}$ (−·−) and ITO/SnO_2/**P** (··■··) electrodes on applied bias.

SCHEME 3

$$\mathbf{P\text{-}C_{60}} \xrightarrow{h\nu} \mathbf{P\text{-}{}^1C_{60}} \quad \text{(a)}$$

$$\mathbf{P\text{-}{}^1C_{60}} \longrightarrow \mathbf{P^{+\bullet}\text{-}C_{60}^{-\bullet}} \quad \text{(b)}$$

$$\mathbf{P^{+\bullet}\text{-}C_{60}^{-\bullet}} + SnO_2 \longrightarrow \mathbf{P^{+\bullet}\text{-}C_{60}} + SnO_2\,(e^-) \quad \text{(c)}$$

$$\mathbf{P^{+\bullet}\text{-}C_{60}} + H_2Q \longrightarrow \mathbf{P\text{-}C_{60}} + HQ^{\bullet} + H^+ \quad \text{(d)}$$

electrodes are irradiated with light of $\lambda < 400$ nm involve the formation of the $\mathbf{P^{+\bullet}}-\mathbf{C_{60}^{-\bullet}}$ photoinduced state (Scheme 3). This is probably a long lifetime charge-transfer state, as it is know[70] for other porphyrin−fullerene dyads in condensed phase.

Moreover, since the oxidation potential of $\mathbf{C_{60}}$ radical anion is ≈−0.57 V versus Ag/AgCl, around 0.3 V less positive than the flat band potential of the semiconductor, the electron injection process (step c, Scheme 3) is exergonic.

Dependence of the Photocurrent on the Applied Potential. The effect of the applied potential on the observed photocurrent generation is shown in Figure 11 for both ITO/SnO_2/**P**−$\mathbf{C_{60}}$ and ITO/SnO_2/**P** electrodes. In this figure, the value of the charge injection yield (Φ_{inj}) from the excited dyes to the semiconductor times the charge collection efficiency, η_c, of the systems[71,72] at the Soret bands are plotted versus the applied potential. These parameters can be obtained from IPCE and the light-harvesting efficiency (LHE = $1-10^{-A}$) of the dye,[72] eq 2.

$$\Phi_{inj}\,\eta_c = \text{IPCE/LHE} \quad (2)$$

The product $\Phi_{inj}\,\eta_c$ increases with anodic bias in both cases, mainly because of the increase in the collection efficiency of the injected electrons.[17,42,73] When the excited sensitizer injects electrons into the SnO_2 particle, the trapped electrons hop through the film to the ITO conducting surface being the driving force for the electric field produced by the applied bias.[42]

Figure 11 also shows that the value of $\Phi_{inj}\,\eta_c$ in $\mathbf{P}-\mathbf{C_{60}}$ dyad is around twice the one obtained with the porphyrin, despite the fact that in the dyad most of the light is adsorbed by the porphyrin moiety. However, the lack of fluorescence from the porphyrin in the dyad (both in solution and in adsorbed state)

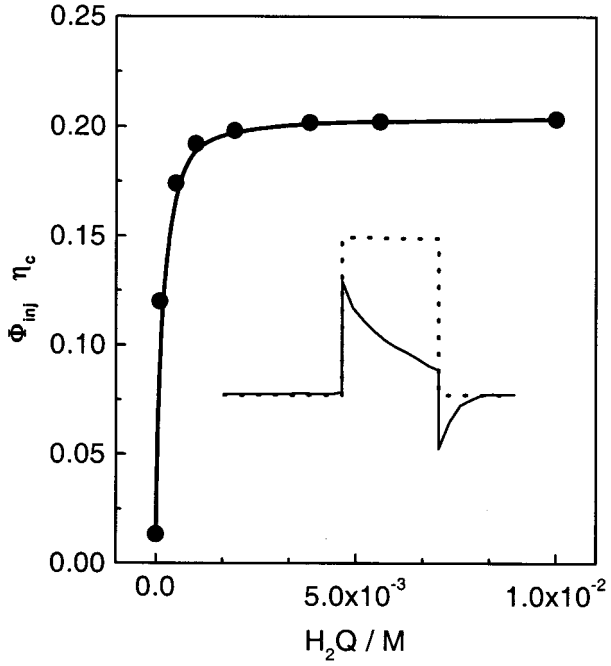

Figure 12. Photocurrent quantum yield of an ITO/SnO_2/$\mathbf{P}-\mathbf{C_{60}}$ electrode as function of the H_2Q concentration. Inset: On−off illumination cycles of photocurrent in precence (·····) and absence (x 10 −) of H_2Q. (Photocurrent was obtained at 0.2 anodic bias vs Ag/AgCl and at the maximum of Soret band.)

SCHEME 4

$$\mathbf{P\text{-}C_{60}} \xrightarrow{h\nu} \mathbf{{}^1P\text{-}C_{60}} \quad \text{(a)}$$

$$\mathbf{{}^1P\text{-}C_{60}} + SnO_2 \longrightarrow \mathbf{P^{+\bullet}\text{-}C_{60}} + SnO_2\,(e^-) \quad \text{(b)}$$

$$\mathbf{{}^1P\text{-}C_{60}} \longrightarrow \mathbf{P^{+\bullet}\text{-}C_{60}^{-\bullet}} \quad \text{(c)}$$

$$\mathbf{P^{+\bullet}\text{-}C_{60}^{-\bullet}} + SnO_2 \longrightarrow \mathbf{P^{+\bullet}\text{-}C_{60}} + SnO_2\,(e^-) \quad \text{(d)}$$

$$\mathbf{P^{+\bullet}\text{-}C_{60}} + H_2Q \longrightarrow \mathbf{P\text{-}C_{60}} + HQ^{\bullet} + H^+ \quad \text{(e)}$$

$$\mathbf{P^{+\bullet}\text{-}C_{60}^{-\bullet}} + H_2Q \longrightarrow \mathbf{P\text{-}C_{60}^{-\bullet}} + HQ^{\bullet} + H^+ \quad \text{(f)}$$

$$\mathbf{P\text{-}C_{60}^{-\bullet}} + SnO_2 \longrightarrow \mathbf{P\text{-}C_{60}} + SnO_2\,(e^-) \quad \text{(g)}$$

indicates that intramolecular charge transfer can compete with the electron-transfer process to the semiconductor. Thus, it is possible that part of the photocurrent is being generated from the $\mathbf{P^{+\bullet}}-\mathbf{C_{60}^{-\bullet}}$ photoinduced charge-separation state. According to the results obtained when both moieties (porphyrin and fullerene) in the dyad are irradiated in the photoelectrochemical cell and according to the photophysical properties of $\mathbf{P}-\mathbf{C_{60}}$, the mechanism shown in Scheme 4 is proposed.

After excitation of the **P** moiety in the dyad (step a, Scheme 4), it can either inject an electron in SnO_2 conduction band (step b) or through a charge-transfer mechanism produce the $\mathbf{P^{+\bullet}}-\mathbf{C_{60}^{-\bullet}}$ state (step c). The intramolecular charge-separation state in turn can either take an electron from the sacrificial donor H_2Q (step f) or inject a charge into the semiconductor (step d). The $\mathbf{P^{+\bullet}}-\mathbf{C_{60}}$ cation formed in steps b and d is reduced by the electron donor (step e). When H_2Q is absent, the anodic photocurrent is small and decreases with the illumination time, and a small cathodic current is observed when the light is turned off, as the oxidized sensitizer (the porphyrin moiety, Scheme 4) retraps photoinjected electrons (see inset in Figure 12). In the presence of H_2Q, higher stationary anodic photocurrent is observed during illumination, and the cathodic current is

suppressed. The increase of the sacrificial donor (H_2Q) concentration present in the electrolyte improves the efficiency of photocurrent generation (Figure 12), as is predicted by the mechanism proposed in Scheme 4. Finally, the $\mathbf{P-C_{60}}^{-\bullet}$ anion formed in the presence of H_2Q in step f can inject charge in the SnO_2 conduction band (step g).

From the analysis of the proposed mechanism in Scheme 4, one can observe that the heterogeneous charge-transfer process shown in steps b and d both produce the porphyrin radical cation. Thus, the back-electron-transfer process of steps b and d would involve the reduction of this cation, while this deleterious process for the photocurrent efficiency in step g would involve the reduction of the uncharged dyad. Thus, a possible reason for the higher photocurrent efficiency in the dyad, in comparison with the porphyrin monomer under the same experimental conditions, could be the contribution of steps d, f, and g in the observed photoelectric effect. The steps preclude back-electron-transfer process, which showed to be the major limiting factor in achieving high IPCE values, producing low efficiency of photon-to-photocurrent conversion.[38,42] The photocurrent generation efficiency for ITO/SnO_2/$\mathbf{P-C_{60}}$ electrode, taken both at the Soret and at the Q-bands, where only the porphyrin moiety absorbs, is always around 2 times higher than in the ITO/SnO_2/**P** electrode. If there were no effects of the presence of $\mathbf{C_{60}}$ moiety in the dyad, both photocurrents should be near the same. Imahori et al.[59,70] have also proposed the formation of an intramolecular charge-transfer process as a previous step in the generation of large photoelectric effect using self-assemble monolayers of ferrocene−porphyrin−fullerene triads. Moreover, a similar mechanism has been recently proposed for the photocurrent generation in nanostructured thin films of porphyrin−fullerene dyads.[21,74]

4. Conclusions

A phorphyrin−fullerene dyad molecule has been synthesized and characterized through electrochemical and photochemical studies. This dyad showed to be effective in the spectral sensitization of wide band gap nanostructured semiconductor electrode, producing anodic photocurrents and photovoltage under visible irradiation. Regardless that the porphyrin fluorescence is strongly quenched by the $\mathbf{C_{60}}$ moiety in the dyad, the photocurrent generation quantum yield is around twice in the dyad when it is compared with the same yield of the porphyrin moiety. The mechanism involving the formation of an intramolecular photoinduced charge-transfer state is proposed to explain the photocurrent produced by excitation of $\mathbf{C_{60}}$ moiety and the higher efficiency in the generation of photoelectrical effect when the incident light is absorbed by the porphyrin moiety in the dyad.

Acknowledgment. We are grateful to Consejo Nacional de Investigaciones Científicas y Técnicas (CONICET-Argentina), Agencia Nacional de Promoción Científica y Tecnológica (FONCYT-Argentina), and Secretaría de Ciencia y Técnica de la Universidad Nacional de Río Cuarto (SECYT-UNRC) for financial support. F. Fungo thanks CONICET for a research fellowship. C. D. Borsarelli and E. Durantini thank Fundacion Antorchas for financial support.

References and Notes

(1) Gust, D.; Moore, T. *Top. Curr. Chem.* **1991**, *159*, 103.
(2) Kuciauskas, D.; Liddell, P. A.; Lin, S.; Johnson, T. E.; Weghorn, S. J.; Lindsey, J. S.; Moore, A. L.; Moore, T. A.; Gust, D. *J. Am. Chem. Soc.* **1999**, *121*, 8604.
(3) Wasielewski, M. R. *Chem. Rev.* **1992**, *92*, 435.
(4) Springs, S. L.; Gosztola, D.; Wasielewski, M. R.; Král, V.; Andrievsky, A.; Sessler, J. L. *J. Phys. Chem.* **1999**, *121*, 2281.
(5) Hirsch, A. *The Chemistry of the Fullerenes*; Thieme: Stuttgart, 1994.
(6) Diederich, F.; Isaacs, L.; Philp, D. *Chem. Soc. Rev.* **1994**, 243.
(7) Fox, M. A.; Pan, H. L.; Jones, W.; Melamed, D. *J. Phys. Chem.* **1995**, *99*, 11523.
(8) Kay, A.; Humphry-Baker, R.; Grätzel, M. *J. Phys. Chem.* **1994**, *98*, 952.
(9) Bedja, I.; Kamat, P. V.; Hotchandani, S. *J. Appl. Phys.* **1996**, *80*, 4637.
(10) Deng, H.; Mao, H.; Lu, Z.; Li, J.; Xu, H. *J. Photochem. Photobiol., A* **1997**, *110*, 47.
(11) Otero, L.; Osora, H.; Li, W.; Fox, M. A. *J. Porphyrins Phthalocyanines* **1998**, *2*, 123.
(12) Deng, H. H.; Lu, Z. H. *Supramol. Sci.* **1998**, *5*, 669.
(13) Wienke, J.; Schaafsma, T. J.; Goossens, A. *J. Phys. Chem. B* **1999**, *103*, 2702.
(14) Shimizu, Y.; Higashiyama, T.; Fuchita, T. *Thin Solid Films* **1998**, *331*, 279.
(15) Fermin, D. J.; Ding, Z. F.; Duong, H. D.; Brevet, P. F.; Girault, H. H. *J. Phys. Chem. B* **1998**, *102*, 10334.
(16) Takahashi, K.; Goda, T.; Yamaguchi, T.; Komura, T.; Murata, K. *J. Phys. Chem. B* **1999**, *103*, 4868.
(17) Tachivana, Y.; Haque, S. A.; Mercer, I. P.; Durrant, J. R.; Klug, D. R. *J. Phys. Chem. B* **2000**, *104*, 1198.
(18) Liu, C. Y.; Bard, A. J. *Acc. Chem. Res.* **1999**, *32*, 235.
(19) Fungo, F.; Otero, L.; Sereno, L.; Silber, J. J.; Durantini, E. N. *J. Mater. Chem.* **2000**, *10*, 645.
(20) Fungo, F.; Otero, L.; Durantini, E. N.; Silber, J. J.; Sereno, L. E. *J. Phys. Chem. B* **2000**, *104*, 7644.
(21) Fungo, F.; Otero, L.; Sereno, L.; Silber, J. J.; Durantini, E. N. *Dyes Pigm.* **2001**, *50*, 163.
(22) Koehorst, R. V.; Boscholoo, G. K.; Savenije, T. J.; Goossens, A.; Schaafsma, T. J. *J. Phys. Chem. B* **2000**, *104*, 2371.
(23) Land, E. J.; Lexa, D.; Bensasson, R. V.; Gust, D.; Moore, T. A.; Moore, A. L.; Liddell, P. A.; Nemeth, G. A. *J. Phys. Chem.* **1987**, *91*, 4831.
(24) Peychal-Heiling, G.; Wilson, G. S. *Anal. Chem.* **1971**, *43*, 545.
(25) Gust, D.; Moore, T.; Moore, A.; Gao, F.; Luttrull, D.; DeGrazaino, J.; Ma, X.; Makings, L.; Lee, S.-J.; Trier, T.; Bittersmann, E.; Seely, G.; Woodward, S.; Bensansson, R.; Rougée, M.; De Schryver, F.; Van der Auweraer, M. *J. Am. Chem. Soc.* **1991**, *113*, 3638.
(26) Kadish, K. M.; Guo, N.; Caemelbecke, E. V.; Paolesse R.; Monti, D.; Tagliatesta, P. *J. Porphyrins Phthalocyanines* **1998**, *2*, 439.
(27) Kuciauskas, D.; Lin, S.; Seely, G. R.; Moore, A. L.; Moore, T. A.; Gust, D.; Drovetskaya, T.; Reed, C. A.; Boyd, P. D. *J. Phys. Chem.* **1996**, *100*, 15926.
(28) Baran, P. S.; Monaco, R. R.; Khan, A. U.; Schuster, D. I.; Wilson, S. R. *J. Am. Chem. Soc.* **1997**, *119*, 8363.
(29) Cheng, T.; Wilson, S. R.; Schuster, D. I. *Chem. Commun.* **1999**, 89.
(30) Da Ros, T.; Prato, M.; Guldi, D.; Alessio, E.; Ruzzi, M.; Pasimeni, L. *Chem. Commun.* **1999**, 635.
(31) Tkachenko, N. V.; Rantala, L.; Tauber, A. Y.; Helaja, J.; Hynninen, H.; Lemmetyinen, H. *J. Am. Chem. Soc.* **1999**, *121*, 9378.
(32) D'Souza, F.; Deviprasad, G.; El-Khouly, M. E.; Fujitsuka, M.; Ito, O. *J. Am. Chem. Soc.* **2001**, *123*, 5277.
(33) Takahashi, K.; Etoh, K.; Tsuda, Y.; Yamaguchi, T.; Komura, T.; Ito, S.; Murata, K. *J. Electroanal. Chem.* **1997**, *426*, 85.
(34) Memming, R. *Comprehensive Treatise of Electrochemistry*; Plenum Press: New York, 1983; Chapter 7, p 529.
(35) Gerischer, H.; Willig, F. *Top. Curr. Chem.* **1976**, *61*, 31.
(36) Cahen, D.; Hodes, G.; Grätzel, M.; Guillemoles, J. F.; Riess, I. *J. Phys. Chem.* **2000**, *104*, 2053.
(37) O'Regan, B.; Grätzel, M. *Nature (London)* **1991**, *353*, 737.
(38) Nasr, C.; Kamat, P. V.; Hotchandani, S. *J. Phys. Chem. B* **1998**, *102*, 10047.
(39) Hagfeld, A.; Grätzel, M. *Chem. Rev.* **1995**, *95*, 49.
(40) Kamat, P. V. *Prog. React. Kinet.* **1994**, *19*, 277.
(41) Kamat, P. V. *CHEMTECH* **1995**, *25*, 22.
(42) Haque, S. A.; Tachivana, Y.; Willis R. L.; Moser, J. E.; Grätzel, M.; Klug, D. R.; Durrant, J. R. *J. Phys. Chem B* **2000**, *104*, 538.
(43) Kamat, P. V.; Barazzouk, K.; Thomas, G.; Hotchandani, S. *J. Phys. Chem. B* **2000**, *104*, 4014.
(44) Durantini, E. N.; Silber, J. J. *Synth. Commun.* **1999**, *29*, 3353.
(45) Isaacs, L.; Diederich, F. *Helv. Chim. Acta* **1993**, *76*, 1231.
(46) Dewar, M. J.; Zoebisch, E. G.; Healy, E. F.; Stewart, J. J. *J. Am. Chem. Soc.* **1985**, *107*, 3902.
(47) Bedja, I.; Hotchandani, S.; Kamat, P. V. *J. Phys. Chem.* **1994**, *98*, 4133.
(48) Borsarelli, C: D.; Cosa, J. J.; Previtali, C. M. *Photochem. Photobiol.* **1998**, *68*, 438.

(49) Borsarelli, C. D.; Durantini, E. N.; García, N. A. *J. Chem. Soc., Perkin Trans. 2* **1996**, 2009.
(50) Echegoyen, L.; Echegoyen, L. E. *Acc. Chem. Res.* **1998**, *31*, 593.
(51) Ottolenghi, M. *Acc. Chem. Res.* **1973**, *6*, 153.
(52) Weller, A.; Staerk, H.; Schomburg, H. *Acta Phys. Pol.* **1987**, *A71*, 707.
(53) Harriman, A. *J. Chem. Soc., Faraday Trans. 1* **1980**, *76*, 1978.
(54) Hung, R. R.; Grabowski, J. J. *J. Phys. Chem.* **1991**, *95*, 6073.
(55) Imahori, H.; Tamaki, K.; Guldi, D. M.; Luo, C.; Fujitsuka, M.; Ito, O.; Sakata, Y.; Fukuzumi, S. *J. Am. Chem. Soc.* **2001**, *123*, 2607.
(56) Imahori, H.; El-Khouly, M. E.; Fujitsuka, M.; Ito, O.; Sakata, Y.; Fukuzumi, S. *J. Phys. Chem. A* **2001**, *105*, 325.
(57) Kuciauskas, D.; Liddell, P. A.; Lin, S.; Stone, S. G.; Moore, A. L.; Moore, T. A.; Gust, D. *J. Phys. Chem. B* **2000**, *104*, 4307.
(58) Imahori, H.; Tkachenko, N.; Vehmanen V.; Tamaki, K.; Lemmetyinen, H.; Sakata, Y.; Fukuzumi, S. *J. Phys. Chem. A* **2001**, *105*, 1750.
(59) Imahori, H.; Norieda, H.; Yamada, H.; Nishimura, Y.; Yamazaki, I.; Sakata, Y.; Fukuzumi, S. *J. Am. Chem. Soc.* **2001**, *123*, 100.
(60) Redmond, R.; Gamlin, J. N. *Photochem. Photobiol.* **1999**, *70*, 391.
(61) Liddell, P.; Macpherson, A. N.; Sumida, J.; Demanche, L.; Moore, A. L.; Moore, T. A.; Gust, D. *Photochem. Photobiol.* **1994**, 59S, 36S.
(62) Imahori, H.; Hagiwara, K.; Aoki, M.; Akiyama, T.; Taniguchi, S.; Okada, T.; Shirakawa, M.; Sakata, Y. *J. Am. Chem. Soc.* **1996**, *118*, 11771.
(63) Imahori, H.; Sakata, Y. *Eur. J. Chem.* **1999**, 2445.
(64) Tkanchenko, N. V.; Gunther, C.; Imahori, H.; Tamaki, K.; Sakata, Y.; Fukuzumi, S.; Lemmetyinen, H. *Chem. Phys. Lett.* **2000**, *326*, 344.
(65) Vlachopoulos, P.; Liska, P.; Augustynski, J.; Grätzel, M. *J. Am. Chem. Soc.* **1988**, *110*, 1216.
(66) Lou, C.; Huang, C.; Liangbing, G.; Zhou, D.; Xia, W.; Zhuang, Q.; Zhao, Y.; Huang, Y. *J. Phys. Chem.* **1996**, *100*, 16685.
(67) Zhang, W.; Shi, Y.; Liangbing, G.; Huang, C.; Lou, H.; Wu, D.; Li, N. *J. Phys. Chem. B* **1999**, *103*, 675.
(68) Cox, D. M.; Trevor, D. J.; Reichmann, K. C.; Kaldor, A. *J. Am. Chem. Soc.* **1991**, *113*, 777.
(69) Dubois, D.; Kadish, K.; Flanagan, S.; Wilson, L. J. *J. Am. Chem. Soc.* **1986**, *108*, 2457.
(70) Imahori, H.; Yamada, H.; Nishimura, Y.; Yamazaki, I.; Sakata, Y. *J. Phys. Chem. B* **2000**, *104*, 2099.
(71) Nazeeruddin, M. K.; Kay, A.; Rodicio, I.; Humphry-Baker, R.; Muller, E.; Liska, P.; Vlachopoulus, N.; Grätzel, M. *J. Am. Chem. Soc.* **1993**, *115*, 6382.
(72) Bedja, I.; Kamat, P. V.; Hua, X.; Lappin, A. G.; Hotchandani, S. *Langmuir* **1997**, *13*, 2398.
(73) Li, W.; Osora, H.; Otero, L.; Duncan, D. C.; Fox, M. A. *J. Phys. Chem. B* **1998**, *102*, 5333.
(74) Imahori, H.; Hasobe, T.; Yamada, H.; Kamat, P. V.; Barazzouk, S.; Fujitsuka, M.; Ito, O.; Fukuzumi, S. *Chem. Lett.* **2001**, *8*, 784.